



## Analyzing the MHD boundary layer flow of Rivlin-Ericksen fluid over a stretching sheet by applying the Taylor wavelet approach

Prithvi Suresh, Vidya Shree Ramareddy, and Patil Mallikarjun Basavaraj\*

Department of Studies and Research in Mathematics, Tumkur University, Tumkur-572103, Karnataka, India.

### Abstract

In the current paper, we newly established the Taylor wavelet operational matrix method to study Rivlin-Ericksen fluid flowing over the stretching sheet in the context of a magnetic field. The Taylor wavelet operational matrix method is a newly devised method for transforming the nonlinear differential equations to nonlinear algebraic equations. This computation is flexible and facile due to the generation of integral matrices. From these integral matrices, unresolved Taylor wavelet coefficients are determined with the help of solvers. Thus, the solution to the given Rivlin-Ericksen fluid flow is achieved. This analysis examines the MHD Rivlin-Ericksen fluid flowing in the steady state caused by stretching a sheet while accounting for the inverse Darcy model. The aforementioned computational method is for seeking solutions to ordinary differential equations. Firstly, the momentum equation is changed to an ordinary differential equation by employing the similarity transformation, and then Taylor wavelet method has to be implemented for further analysis. The effect of the viscoelastic parameter, inverse Darcy number, magnetic parameter, and inclination angle on axial and transverse velocity are taken into consideration for study analysis. Engineering application tool local skin friction coefficient variation has been assessed for different parameters, and the estimated local skin friction coefficient is compared with bvp4c, demonstrating the compatibility of the Taylor wavelet approach.

**Keywords.** Operational integration matrix, Rivlin-Erickson fluid, Taylor wavelet, Stretching sheet, Collocation method.

**2010 Mathematics Subject Classification.** 65L05, 34K06, 34K28.

### 1. INTRODUCTION

The industrial applications of making plastic sheets from synthetic materials are expanding on a daily basis, necessitating the description of the intrinsic phenomena involved. Numerical output for the momentum equation obtained through the wavelet method has been benchmarked with the exact solution as the validation procedure. The theoretical model was first developed for a particular fluid known as Rivlin-Erickson fluid by Rivlin-Erickson [19], and the elasticity of the material has been explored with the help of a single-valued energy strain function. The effect of Rivlin-Erickson fluid flow over the boundary has been evaluated by Siddappa and Khapate [26], which is an extension of Crane's [3] work. The importance of studying the non-Newtonian fluid is that it has a wide range of applications, such as communication devices, industrial applications, agricultural areas, and biomedical devices.

There are several non-Newtonian fluids, such as Williamson fluid, Casson fluid, etc. Among them, Rivlin-Erickson fluid is one such fluids that has been used in tires, ceramic materials, foams, and filtration processes, etc. Sharma and Kumar [21] have shown the stabilizing impact of the rotation on Rivlin-Erickson fluid flow. The Laplace transform method has been implemented to obtain the exact solution of second-grade Rivlin-Erickson fluid flow for Rayleigh's problem by Jordan and Puri [8] and has observed the steady-state configuration due to discontinuity arising in the beginning. With the help of the dispersion equation stability analysis has been made for viscoelastic fluid by Kumar and Singh [12]. Shukla and Awasthi [24] explored wave number and Perturbation growth variation and visualized

Received: 29 May 2024; Accepted: 20 January 2025.

\* Corresponding author. Email: mbp1007@yahoo.com.

it in the form of graphs. They have assessed that the interface becomes unstable when thickness grows through the Newton-Raphson method.

Pradeep *et al.* [11] have inferred that there is both a stabilizing and destabilizing effect in the presence of a magnetic field and a stabilizing effect on rotating the viscoelastic fluid. Kareem *et al.* [9] solved the energy balance and momentum equations by the finite difference method and inferred that a lower dissipation rate minimizes the entropy production. Convection of oscillatory and non-oscillatory systems for various parameters such as kinematic number, Vadasz number, and Lewis number has been studied by Chand and Rana [2]. Slemrod [27] has expressed polymeric fluids as a function of the Rivlin-Erickson tensor. Top-heavy and bottom-heavy configuration have been explained by Sharma *et al.* [22], and they observed Kelvin-Helmholtz instability in the presence of surface tension for Rivlin-Erickson fluid embedded with porous media.

Gupta *et al.* [7] have investigated suspended particles and hall current impact of elastico-viscous fluid and analyzed the stability by linearizing the hydromagnetic perturbed equations. considered steady mass flux over a semi-infinite plate to study the impact of thermal diffusion and diffusion-thermo for Rivlin-Erickson fluid. Reddy *et al.* [18]. Dharamendra *et al.* [5] have comparatively studied the stability of the viscous fluid-viscous fluid interface and the Rivlin-Erickson fluid-viscous fluid interface, concluding that the viscous fluid-viscous fluid interface is less stable compared to the Rivlin-Erickson fluid-viscous fluid interface. Moatimid and Sayed [15] plotted stability plots for various parameters and investigated stability for two Rivlin-Erickson fluids having a cylindrical interface. Prescribed heat flux and prescribed temperature cases are analyzed by making use of Kummer's function, and hence the closed form of the analytical solution is obtained by Vishalakshi *et al.* [32]. Akbar *et al.* [1] analyzed the effect of magnetic fields on the flow of Eyring-Powell fluid and found that increased Eyring-Powell parameters and magnetic field parameters decrease the fluid velocity.

Time signals are monitored and evaluated due to their applications in various systems. For stationary time signals, Joseph Fourier in 1807 developed a transform known as the Fourier Transform. Alfred Haar in 1909 found out the transform for non-stationary signals, and Haar was the one who first called this transform the wavelet transform. Keshavarz *et al.* [10] pioneered the Taylor wavelet generation for solving initial and boundary valued problems. Error analysis has been done for the Benjamin-Bona-Mahony partial differential equation by Shiralashetti and Hanaji [23]. Ratish and Mehra [17] used the Taylor wavelet Galerkin scheme to solve Burger's equation by separating the diffusion and advection terms. Orthonormality of the Taylor wavelet has been considered by Sevin [6] to obtain a solution for the Lane-Emden equations. The Riemann-Liouville fractional integral equation has been explored by Toan *et al.* [28].

Substantial research work has been carried out in wavelets for obtaining solutions in the field of fluid dynamics. The undershoots and overshoots of a viscous fluid in the presence of a magnetic field have been studied with the help of the Bernoulli collocation method by Vivek and Kumar [33]. Vidyashree *et al.* [29] employed the Legendre wavelet operational matrix method to explore the impact of the magnetic and pressure gradient parameters on the boundary layer thickness for the fluid flowing over a stretching sheet. Equations arising in fluid dynamics and astrophysics, such as Emden-Fowler-type equations, have been tackled by the Fibonacci wavelet method by Manohara and Kumbinarasaiah [14]. The effect of Casson parameter and the Grashof and Biot numbers on entropy generation for the Casson fluid flowing in a vertical channel has been discussed by Vidyashree *et al.* [16]. Some other research work has also been carried out in the fluid dynamics field recently [4, 20, 25, 30, 31].

The current investigation aims to enhance Vishalakshi *et al.*'s [32] work by incorporating the newly constructed Taylor wavelet operational matrix. The innovative aspect of this work is the application of the Taylor wavelet approach to solve the nonlinear momentum equation of Rivlin-Erickson fluid flowing past the stretching sheet. Skin friction and the Nusselt number were examined. The impact of various physical characteristics is investigated via graphical representation. Various works have been carried out related to Rivlin-Erickson fluid flow; none of them have been solved using the wavelet method as per the literature survey. This makes the current study more significant and interesting.



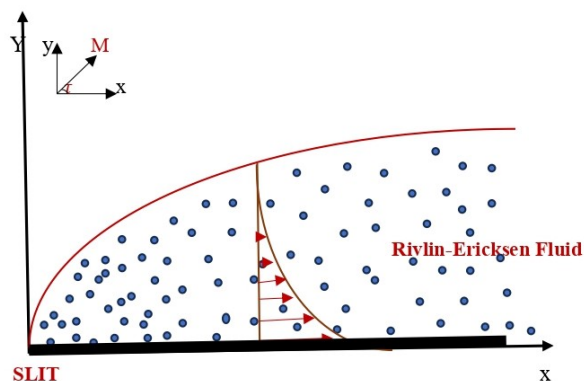


FIGURE 1. Rivlin-Ericksen fluid past a stretching sheet.

2. MATHEMATICAL MODEL AND FORMULATION

This work examines the consistent two-dimensional MHD flow of an electrically operating, incompressible Rivlin-Ericksen fluid over a porous stretching/shrinking sheet with the inverse Darcy model, as depicted in Figure 1. The flow is studied in the presence of an inclined magnetic field. This extends the work of Siddappa and Hiremath [25].

Maxwell’s equation for the flow [32]

$$\vec{J} = \mu_m \sigma (\vec{q} \times \vec{B}), \tag{2.1}$$

$$\nabla \cdot \vec{B} = 0, \tag{2.2}$$

$$\nabla \times \vec{B} = \sigma E_{induced}, \tag{2.3}$$

$$\nabla \times E_{induced} = -\mu_m \frac{\partial \vec{B}}{\partial t}. \tag{2.4}$$

Porous media is injected into the fluid flow, and a homogeneous inclined magnetic field of strength  $B_0$  is applied. The Lorentz force for electrically weak conducting fluid is  $\mu_m \vec{J} \times \vec{B} \sin^2 \tau$ , which results in

$$\mu_m \vec{J} \times \vec{B} \sin^2 \tau = -\mu^2 \sigma B_0^2 \sin^2 \tau u. \tag{2.5}$$

As per the above consideration, the governing boundary layer equation [32] is

$$\frac{\partial u}{\partial x} + \frac{\partial u}{\partial y} = 0, \tag{2.6}$$

$$u \frac{\partial u}{\partial x} + v \frac{\partial u}{\partial y} = \nu \frac{\partial^2 u}{\partial y^2} + k_1 \left[ \left( u \frac{\partial u}{\partial x} + v \frac{\partial u}{\partial y} \right)_{yy} + 2 \left( \frac{\partial u}{\partial x} \frac{\partial u}{\partial y} \right)_y \right] + \gamma \left( \left( \frac{\partial u}{\partial y} \right)^2 \right)_x - \left( \frac{\sigma B_0^2 \sin^2(\tau)}{\rho} + \frac{\mu}{\rho K} \right) u, \tag{2.7}$$

complementing boundary conditions [4]

$$v = 0, \quad u = ax, \quad \text{at } y = 0, \tag{2.8}$$

$$u \rightarrow 0, \quad \frac{\partial u}{\partial y} \rightarrow 0, \quad \text{as } y \rightarrow \infty, \tag{2.9}$$

similarity transformation to nondimensionalize the above equations

$$u = ax f'(\eta), \quad v = -\sqrt{a\nu} f, \quad \text{and } \eta = \sqrt{\frac{a}{\nu}} y. \tag{2.10}$$

Substituting Eq. (2.10) in Eq. (2.7), we obtain the ordinary differential equation

$$f'^2 - f f'' - f''' - \beta(2f' f''' + 3f''^2 - f f'''' ) - 2\gamma f''^2 + (M \sin^2(\tau) + Da^{-1}) f' = 0, \tag{2.11}$$



corresponding boundary conditions reduce to

$$f(0) = 0, f'(0) = 1, f'(\infty) \rightarrow 0, \text{ and } f''(\infty) \rightarrow 0, \tag{2.12}$$

where  $M = \frac{\sigma B_0^2}{\rho a}$ ,  $\beta = \frac{k_1 a}{\gamma}$ , and  $Da^{-1} = \frac{\mu}{\rho a K}$ .

The local skin friction coefficient is  $Cf_x = \frac{\tau_w}{\rho u_\infty^2}$ , where  $\tau_w$  is wall shear stress.

$$Re_x^{\frac{1}{2}} Cf_x = (1 - 3\beta)f''(0). \tag{2.13}$$

### 3. TAYLOR WAVELET AND ITS OPERATIONAL MATRIX

**Definition 3.1** (Taylor wavelet [10]). The Taylor wavelet function over the interval  $[0, 1)$  with  $v$  being the set of all natural numbers up to  $V - 1$  along with zero,  $u = 1$  to  $2^{l-1}$ , and  $l \in Z^+$  is defined as follows:

$$\xi_{u,v}(q) = \begin{cases} 2^{-\frac{1+l}{2}} \bar{\xi}_v(2^{-1+l}q + 1 - u), & \text{if } 2^{\frac{u-1}{2l-1}} \leq q \leq 2^{\frac{u}{2l-1}}, \\ 0, & \text{Otherwise,} \end{cases} \tag{3.1}$$

with  $\bar{\xi}_v(q) = \frac{\xi_v(q)}{\sqrt{2n+1}}$ , where  $\xi_v(q) = q^v$ .

**Approximating function.** Expressing  $F(q)$  in terms of the Taylor wavelet basis is

$$F(q) \approx \sum_{u=1}^{\infty} \sum_{v=1}^{\infty} R_{u,v} \xi_{u,v}(q), \tag{3.2}$$

$$F(q) \approx \sum_{u=1}^{2^{l-1}} \sum_{v=0}^{V-1} R_{u,v} \xi_{u,v}(q) = R^T T_y(q), \tag{3.3}$$

where  $R$  and  $T_y(q)$  are  $2^{l-1}V \times 1$  matrices,

$$R = [R_{1,0} \dots R_{1,V-1} \ R_{2,0} \dots R_{2,V-1} \dots R_{2^{l-1},V-1}],$$

and

$$T_y(q) = [\xi_{1,0} \dots \xi_{1,V-1} \ \xi_{2,0} \dots \xi_{2,D-1} \dots \xi_{2^{l-1},V-1}].$$

For  $V = 10$  and  $l = 1$ , the Taylor wavelet basis is fetched which is given as follows:

$\xi_{1,0}(q) = 1,$	$\xi_{1,1}(q) = \sqrt{3}q,$
$\xi_{1,2}(q) = \sqrt{5}q^2,$	$\xi_{1,3}(q) = \sqrt{7}q^3,$
$\xi_{1,4}(q) = 3q^4,$	$\xi_{1,5}(q) = \sqrt{11}q^5,$
$\xi_{1,6}(q) = \sqrt{13}q^6,$	$\xi_{1,7}(q) = \sqrt{15}q^7,$
$\xi_{1,8}(q) = \sqrt{17}q^8,$	$\xi_{1,9}(q) = \sqrt{19}q^9,$

where  $T_{y10}(q) = [\xi_{1,0} \ \xi_{1,1} \ \xi_{1,2} \ \xi_{1,3} \ \xi_{1,4} \ \xi_{1,5} \ \xi_{1,6} \ \xi_{1,7} \ \xi_{1,8} \ \xi_{1,9}]^T$ .

**Theorem 3.2.** If  $F(q)$  is a bounded continuous function defined in  $H^2[0, 1)$ , then the Taylor wavelet expansion of  $F(q)$  converges to it.

*Proof.* Let  $F(q)$  be a continuous bounded real-valued function defined on  $[0, 1)$ ; then the Taylor coefficients of  $F(q)$  are given as

$$R_{u,v} = \int_0^1 F(q) \xi_{u,v}(q) dq,$$

$$R_{u,v} = \int_I F(q) \frac{2^{\frac{l-1}{2}}}{\sqrt{2u+1}} \xi_v(2^{l-1}q + 1 - u) dx, \text{ where } I = [2^{\frac{u-1}{2l-1}}, 2^{\frac{u}{2l-1}}),$$



substituting  $2^{l-1}q + 1 - u = z$ , we get

$$R_{u,v} = \int_{-1}^1 F\left(\frac{z+u-1}{2^{l-1}}\right) \frac{2^{\frac{l-1}{2}}}{\sqrt{2u+1}} \xi_v(z) 2^{1-l} dz,$$

$$R_{u,v} = \frac{2^{\frac{-l+1}{2}}}{\sqrt{2u+1}} \int_{-1}^1 F\left(\frac{z+u-1}{2^{l-1}}\right) \xi_v(z) dz,$$

by Gauss’s mean value theorem for integrals, we have

$$R_{u,v} = \frac{2^{\frac{-l+1}{2}}}{\sqrt{2u+1}} F\left(\frac{w+u-1}{2^{l-1}}\right) \int_{-1}^1 \xi_v(z) dz, \quad \text{for some } w \in (-1, 1),$$

consider  $\int_{-1}^1 \xi_v(z) dz = g$ , then we get

$$|R_{u,v}| = \left| \frac{2^{\frac{-l+1}{2}}}{\sqrt{2u+1}} \right| \left| F\left(\frac{w+u-1}{2^{l-1}}\right) \right| g.$$

Since  $F(q)$  is a bounded function, hence  $\sum_{u,v=0}^\infty R_{u,v}$  is absolutely convergent. Therefore, the Taylor series expansion converges uniformly □

**Theorem 3.3.** Consider  $F(q) \in C^p[0, 1)$  where  $C^p[0, 1)$ , is a  $p$  times continuously differentiable function, and let  $\xi_{u,v}$  be a Taylor wavelet sequence. Let  $F(q) = \sum_{u=1}^{2^{k-1}} F_u(q)$  and  $f_u(q) = L(\xi_{u,v})$  be the linear space spanned by  $\xi_{u,v}$ . If  $R^T T_y(q)$  is the best approximation from  $f_u(q)$  to  $F_u(q)$ , then  $R^T T_y(q)$  approximates with the following error bound:

$$\|F(q) - R^T T_y(q)\| \leq K \sqrt{\left(\frac{(2^{\frac{u}{2l-1}} - 2^{\frac{u-1}{2l-1}})^{2p+1}}{(2p+1)}\right)}.$$

*Proof.* The Taylor expansion for the function  $F_u(q)$  is

$$\overline{F_u(q)} = F_u(2^{\frac{u-1}{2l-1}}) + F'_u(2^{\frac{u-1}{2l-1}}) \frac{(x - 2^{\frac{u-1}{2l-1}})}{1!} + \dots + F_u^{p-1}(2^{\frac{u-1}{2l-1}}) \frac{(x - 2^{\frac{u-1}{2l-1}})^{p-1}}{(p-1)!},$$

we know that

$$|F_u(q) - \overline{F_u(q)}| \leq |F_u^p(q)| \frac{(x - 2^{\frac{u-1}{2l-1}})^p}{(p!)}, \quad \text{where } q \in [2^{\frac{u-1}{2l-1}}, 2^{\frac{u}{2l-1}}), \tag{3.4}$$

$$\begin{aligned} \|F_u(q) - R^T T_y(q)\|^2 &\leq \|F_u(q) - \overline{F_u(q)}\|^2, \\ \int_{2^{\frac{u-1}{2l-1}}}^{2^{\frac{u}{2l-1}}} |F_u(q) - \overline{F_u(q)}|^2 &\leq \int_{2^{\frac{u-1}{2l-1}}}^{2^{\frac{u}{2l-1}}} \left( |F_u^p(q)| \frac{(x - 2^{\frac{u-1}{2l-1}})^p}{(p!)} \right)^2 dx, \text{ (from Eq. (3.4))} \\ &= \left( \frac{F_u^p(q)}{p!} \right)^2 \left( \frac{(x - 2^{\frac{u-1}{2l-1}})^{2p+1}}{(2p+1)} \right) \Big|_{2^{\frac{u-1}{2l-1}}}^{2^{\frac{u}{2l-1}}}, \\ &= \left( \frac{F_u^p(q)}{p!} \right)^2 \left( \frac{(2^{\frac{u}{2l-1}} - 2^{\frac{u-1}{2l-1}})^{2p+1}}{(2p+1)} \right), \\ &= K \left( \frac{(2^{\frac{u}{2l-1}} - 2^{\frac{u-1}{2l-1}})^{2p+1}}{(2p+1)} \right), \end{aligned} \tag{3.5}$$

where  $K = \left( \frac{F_u^p(q)}{p!} \right)^2$ .



Now, consider

$$\begin{aligned} \|F(q) - R^T T_y(q)\|^2 &\leq \sum_{2^{l-1}}^{u-1} \|F_u(q) - R^T T_y(q)\|^2, \\ \|F(q) - R^T T_y(q)\|^2 &\leq K^2 \left( \frac{(2^{\frac{u}{2^{l-1}}} - 2^{\frac{u-1}{2^{l-1}}})^{2p+1}}{(2p+1)} \right), \\ \|F(q) - R^T T_y(q)\| &\leq K \sqrt{\left( \frac{(2^{\frac{u}{2^{l-1}}} - 2^{\frac{u-1}{2^{l-1}}})^{2p+1}}{(2p+1)} \right)}. \end{aligned}$$

□

**3.1. Operational matrix of integration.** Integrate  $\xi_{u,v}(q)$  with respect to  $q$  and represent it as a linear combination of the Taylor wavelet basis, we get

$$\begin{aligned} \int_0^q \xi_{1,0}(q) dq &= [0 \quad \frac{780}{1351} \quad 0 \quad 0 \quad 0 \quad 0 \quad 0 \quad 0 \quad 0] T_{y10}(q), \\ \int_0^q \xi_{1,1}(q) dq &= [0 \quad 0 \quad \frac{744}{1921} \quad 0 \quad 0 \quad 0 \quad 0 \quad 0 \quad 0] T_{y10}(q), \\ \int_0^q \xi_{1,2}(q) dq &= [0 \quad 0 \quad 0 \quad \frac{282}{1001} \quad 0 \quad 0 \quad 0 \quad 0 \quad 0] T_{y10}(q), \\ \int_0^q \xi_{1,3}(q) dq &= [0 \quad 0 \quad 0 \quad 0 \quad \frac{506}{2295} \quad 0 \quad 0 \quad 0 \quad 0] T_{y10}(q), \\ \int_0^q \xi_{1,4}(q) dq &= [0 \quad 0 \quad 0 \quad 0 \quad 0 \quad \frac{415}{2294} \quad 0 \quad 0 \quad 0] T_{y10}(q), \\ \int_0^q \xi_{1,5}(q) dq &= [0 \quad 0 \quad 0 \quad 0 \quad 0 \quad 0 \quad \frac{595}{3881} \quad 0 \quad 0] T_{y10}(q), \\ \int_0^q \xi_{1,6}(q) dq &= [0 \quad 0 \quad 0 \quad 0 \quad 0 \quad 0 \quad 0 \quad \frac{807}{6068} \quad 0] T_{y10}(q), \\ \int_0^q \xi_{1,7}(q) dq &= [0 \quad 0 \quad 0 \quad 0 \quad 0 \quad 0 \quad 0 \quad 0 \quad \frac{1051}{8951}] T_{y10}(q), \\ \int_0^q \xi_{1,8}(q) dq &= [0 \quad 0 \quad 0 \quad 0 \quad 0 \quad 0 \quad 0 \quad 0 \quad 0 \quad \frac{1327}{12626}] T_{y10}(q), \\ \int_0^q \xi_{1,9}(q) dq &= [0 \quad 0 \quad 0 \quad 0 \quad 0 \quad 0 \quad 0 \quad 0 \quad 0 \quad 0] T_{y10}(q) + \frac{76}{799} \xi_{1,11}(q). \end{aligned}$$

This implies

$$\int_0^q T_{y10}(q) dq = S_{10 \times 10} T_{y10}(q) + \hat{T}_{y10}(q),$$



where

$$S = \begin{bmatrix} 0 & \frac{780}{1351} & 0 & 0 & 0 & 0 & 0 & 0 & 0 & 0 \\ 0 & 0 & \frac{744}{1921} & 0 & 0 & 0 & 0 & 0 & 0 & 0 \\ 0 & 0 & 0 & \frac{282}{1001} & 0 & 0 & 0 & 0 & 0 & 0 \\ 0 & 0 & 0 & 0 & \frac{506}{2295} & 0 & 0 & 0 & 0 & 0 \\ 0 & 0 & 0 & 0 & 0 & \frac{415}{2294} & 0 & 0 & 0 & 0 \\ 0 & 0 & 0 & 0 & 0 & 0 & \frac{595}{3881} & 0 & 0 & 0 \\ 0 & 0 & 0 & 0 & 0 & 0 & 0 & \frac{807}{6068} & 0 & 0 \\ 0 & 0 & 0 & 0 & 0 & 0 & 0 & 0 & \frac{1051}{8951} & 0 \\ 0 & 0 & 0 & 0 & 0 & 0 & 0 & 0 & 0 & \frac{1327}{12626} \end{bmatrix}, \text{ and } \hat{T}_{y10}(q) = \begin{bmatrix} 0 \\ 0 \\ 0 \\ 0 \\ 0 \\ 0 \\ 0 \\ 0 \\ 0 \\ \frac{76}{799} \xi_{1,11}(q) \end{bmatrix}.$$

Integrating  $\xi_{u,v}(q)$  twice with respect to  $q$  and representing it as a linear combination of the Taylor wavelet basis, we have

$$\begin{aligned} \int_0^q \int_0^q \xi_{1,0}(q) dqdq &= [0 \ 0 \ \frac{646}{2889} \ 0 \ 0 \ 0 \ 0 \ 0 \ 0 \ 0] T_{y10}(q)(\xi), \\ \int_0^q \int_0^q \xi_{1,1}(q) dqdq &= [0 \ 0 \ 0 \ \frac{660}{6049} \ 0 \ 0 \ 0 \ 0 \ 0 \ 0] T_{y10}(q), \\ \int_0^q \int_0^q \xi_{1,2}(q) dqdq &= [0 \ 0 \ 0 \ 0 \ \frac{321}{5168} \ 0 \ 0 \ 0 \ 0 \ 0] T_{y10}(q), \\ \int_0^q \int_0^q \xi_{1,3}(q) dqdq &= [0 \ 0 \ 0 \ 0 \ 0 \ \frac{701}{17575} \ 0 \ 0 \ 0 \ 0] T_{y10}(q), \\ \int_0^q \int_0^q \xi_{1,4}(q) dqdq &= [0 \ 0 \ 0 \ 0 \ 0 \ 0 \ \frac{1297}{46764} \ 0 \ 0 \ 0] T_{y10}(q), \\ \int_0^q \int_0^q \xi_{1,5}(q) dqdq &= [0 \ 0 \ 0 \ 0 \ 0 \ 0 \ 0 \ \frac{22}{1079} \ 0 \ 0] T_{y10}(q), \\ \int_0^q \int_0^q \xi_{1,6}(q) dqdq &= [0 \ 0 \ 0 \ 0 \ 0 \ 0 \ 0 \ 0 \ \frac{26}{1665} \ 0] T_{y10}(q), \\ \int_0^q \int_0^q \xi_{1,7}(q) dqdq &= [0 \ 0 \ 0 \ 0 \ 0 \ 0 \ 0 \ 0 \ 0 \ 0 \ \frac{30}{2431}] T_{y10}(q), \\ \int_0^q \int_0^q \xi_{1,8}(q) dqdq &= [0 \ 0 \ 0 \ 0 \ 0 \ 0 \ 0 \ 0 \ 0 \ 0 \ 0] T_{y10}(q) + \frac{34}{3401} \xi_{1,11}(q), \\ \int_0^q \int_0^q \xi_{1,9}(q) dqdq &= [0 \ 0 \ 0 \ 0 \ 0 \ 0 \ 0 \ 0 \ 0 \ 0 \ 0] T_{y10}(q) + \frac{38}{4599} \xi_{1,12}(q). \end{aligned}$$

This implies

$$\int_0^q \int_0^q T_{y10}(q) dqdq = S'_{10 \times 10} T_{y10}(q) + \hat{T}'_{y10}(q),$$

where

$$S' = \begin{bmatrix} 0 & 0 & \frac{646}{2889} & 0 & 0 & 0 & 0 & 0 & 0 & 0 \\ 0 & 0 & 0 & \frac{660}{6049} & 0 & 0 & 0 & 0 & 0 & 0 \\ 0 & 0 & 0 & 0 & \frac{321}{5168} & 0 & 0 & 0 & 0 & 0 \\ 0 & 0 & 0 & 0 & 0 & \frac{701}{17575} & 0 & 0 & 0 & 0 \\ 0 & 0 & 0 & 0 & 0 & 0 & \frac{1297}{46764} & 0 & 0 & 0 \\ 0 & 0 & 0 & 0 & 0 & 0 & 0 & \frac{22}{1079} & 0 & 0 \\ 0 & 0 & 0 & 0 & 0 & 0 & 0 & 0 & \frac{26}{1665} & 0 \\ 0 & 0 & 0 & 0 & 0 & 0 & 0 & 0 & 0 & \frac{30}{2431} \\ 0 & 0 & 0 & 0 & 0 & 0 & 0 & 0 & 0 & 0 \\ 0 & 0 & 0 & 0 & 0 & 0 & 0 & 0 & 0 & 0 \end{bmatrix}, \text{ and } \hat{T}'_{y10}(q) = \begin{bmatrix} 0 \\ 0 \\ 0 \\ 0 \\ 0 \\ 0 \\ 0 \\ 0 \\ 0 \\ \frac{34}{3401} \xi_{1,11}(q) \\ \frac{38}{4599} \xi_{1,12}(q) \end{bmatrix}.$$



Integrating  $\xi_{u,v}(q)$  thrice with respect to  $q$  between and representing it as a linear combination of the Taylor wavelet basis.

$$\begin{aligned} \int_0^q \int_0^q \int_0^q \xi_{1,0}(q) dqdqdq &= [0 \ 0 \ 0 \ \frac{255}{4048} \ 0 \ 0 \ 0 \ 0 \ 0 \ 0]T_{y10}(q), \\ \int_0^q \int_0^q \int_0^q \xi_{1,1}(q) dqdqdq &= [0 \ 0 \ 0 \ 0 \ \frac{65}{2702} \ 0 \ 0 \ 0 \ 0 \ 0]T_{y10}(q), \\ \int_0^q \int_0^q \int_0^q \xi_{1,2}(q) dqdqdq &= [0 \ 0 \ 0 \ 0 \ 0 \ \frac{175}{15841} \ 0 \ 0 \ 0 \ 0]T_{y10}(q), \\ \int_0^q \int_0^q \int_0^q \xi_{1,3}(q) dqdqdq &= [0 \ 0 \ 0 \ 0 \ 0 \ 0 \ \frac{77}{12592} \ 0 \ 0 \ 0]T_{y10}(q), \\ \int_0^q \int_0^q \int_0^q \xi_{1,4}(q) dqdqdq &= [0 \ 0 \ 0 \ 0 \ 0 \ 0 \ 0 \ \frac{46}{12471} \ 0 \ 0]T_{y10}(q), \\ \int_0^q \int_0^q \int_0^q \xi_{1,5}(q) dqdqdq &= [0 \ 0 \ 0 \ 0 \ 0 \ 0 \ 0 \ 0 \ \frac{37}{15455} \ 0]T_{y10}(q), \\ \int_0^q \int_0^q \int_0^q \xi_{1,6}(q) dqdqdq &= [0 \ 0 \ 0 \ 0 \ 0 \ 0 \ 0 \ 0 \ 0 \ \frac{49}{29856}]T_{y10}(q), \\ \int_0^q \int_0^q \int_0^q \xi_{1,7}(q) dqdqdq &= [0 \ 0 \ 0 \ 0 \ 0 \ 0 \ 0 \ 0 \ 0 \ 0]T_{y10}(q) + \frac{17}{60486}\xi_{1,11}(q), \\ \int_0^q \int_0^q \int_0^q \xi_{1,8}(q) dqdqdq &= [0 \ 0 \ 0 \ 0 \ 0 \ 0 \ 0 \ 0 \ 0 \ 0]T_{y10}(q) + \frac{17}{19576}\xi_{1,12}(q), \\ \int_0^q \int_0^q \int_0^q \xi_{1,9}(q) dqdqdq &= [0 \ 0 \ 0 \ 0 \ 0 \ 0 \ 0 \ 0 \ 0 \ 0]T_{y10}(q) + \frac{7}{10599}\xi_{1,13}(q). \end{aligned}$$

This implies

$$\int_0^q \int_0^q \int_0^q T_{y10}(q) dqdqdq = S''_{10 \times 10} T_{y10}(q) + \hat{T}''_{y10}(q),$$

where

$$S'' = \begin{bmatrix} 0 & 0 & 0 & \frac{255}{4048} & 0 & 0 & 0 & 0 & 0 & 0 \\ 0 & 0 & 0 & 0 & \frac{65}{2702} & 0 & 0 & 0 & 0 & 0 \\ 0 & 0 & 0 & 0 & 0 & \frac{175}{15841} & 0 & 0 & 0 & 0 \\ 0 & 0 & 0 & 0 & 0 & 0 & \frac{77}{12592} & 0 & 0 & 0 \\ 0 & 0 & 0 & 0 & 0 & 0 & 0 & \frac{46}{12471} & 0 & 0 \\ 0 & 0 & 0 & 0 & 0 & 0 & 0 & 0 & \frac{37}{15455} & 0 \\ 0 & 0 & 0 & 0 & 0 & 0 & 0 & 0 & 0 & \frac{49}{29856} \\ 0 & 0 & 0 & 0 & 0 & 0 & 0 & 0 & 0 & 0 \\ 0 & 0 & 0 & 0 & 0 & 0 & 0 & 0 & 0 & 0 \\ 0 & 0 & 0 & 0 & 0 & 0 & 0 & 0 & 0 & 0 \end{bmatrix}, \text{ and } \hat{T}''_{y10}(q) = \begin{bmatrix} 0 \\ 0 \\ 0 \\ 0 \\ 0 \\ 0 \\ 0 \\ \frac{17}{60486}\xi_{1,11}(q) \\ \frac{17}{19576}\xi_{1,12}(q) \\ \frac{7}{10599}\xi_{1,13}(q) \end{bmatrix}.$$

Integrating  $\xi_{u,v}(q)$  fourth time with respect to  $q$  and representing it as a linear combination of the Taylor wavelet basis, we get

$$\begin{aligned} \int_0^q \int_0^q \int_0^q \int_0^q \xi_{1,0}(q) dqdqdqdq &= [0 \ 0 \ 0 \ 0 \ \frac{1}{72} \ 0 \ 0 \ 0 \ 0 \ 0]T_{y10}(q), \\ \int_0^q \int_0^q \int_0^q \int_0^q \xi_{1,1}(q) dqdqdqdq &= [0 \ 0 \ 0 \ 0 \ 0 \ \frac{23}{5285} \ 0 \ 0 \ 0 \ 0]T_{y10}(q), \\ \int_0^q \int_0^q \int_0^q \int_0^q \xi_{1,2}(q) dqdqdqdq &= [0 \ 0 \ 0 \ 0 \ 0 \ 0 \ \frac{29}{16834} \ 0 \ 0 \ 0]T_{y10}(q), \end{aligned}$$



$$\begin{aligned} \int_0^q \int_0^q \int_0^q \int_0^q \xi_{1,3}(q)dq dq dq dq &= [0 \ 0 \ 0 \ 0 \ 0 \ 0 \ 0 \ \frac{41}{50415} \ 0 \ 0]T_{y10}(q), \\ \int_0^q \int_0^q \int_0^q \int_0^q \xi_{1,4}(q)dq dq dq dq &= [0 \ 0 \ 0 \ 0 \ 0 \ 0 \ 0 \ 0 \ \frac{16}{36943} \ 0]T_{y10}(q), \\ \int_0^q \int_0^q \int_0^q \int_0^q \xi_{1,5}(q)dq dq dq dq &= [0 \ 0 \ 0 \ 0 \ 0 \ 0 \ 0 \ 0 \ 0 \ \frac{19}{75512}]T_{y10}(q), \\ \int_0^q \int_0^q \int_0^q \int_0^q \xi_{1,6}(q)dq dq dq dq &= [0 \ 0 \ 0 \ 0 \ 0 \ 0 \ 0 \ 0 \ 0 \ 0]T_{y10}(q) + \frac{11}{70463}\xi_{1,11}(q), \\ \int_0^q \int_0^q \int_0^q \int_0^q \xi_{1,7}(\xi)dq dq dq dq &= [0 \ 0 \ 0 \ 0 \ 0 \ 0 \ 0 \ 0 \ 0 \ 0]T_{y10}(q) + \frac{6}{58843}\xi_{1,12}(q), \\ \int_0^q \int_0^q \int_0^q \int_0^q \xi_{1,8}(q)dq dq dq dq &= [0 \ 0 \ 0 \ 0 \ 0 \ 0 \ 0 \ 0 \ 0 \ 0]T_{y10}(q) + \frac{8}{115253}\xi_{1,13}(q), \\ \int_0^q \int_0^q \int_0^q \int_0^q \xi_{1,9}(q)dq dq dq dq &= [0 \ 0 \ 0 \ 0 \ 0 \ 0 \ 0 \ 0 \ 0 \ 0]T_{y10}(q) + \frac{13}{265929}\xi_{1,14}(q). \end{aligned}$$

This implies

$$\int_0^q \int_0^q \int_0^q \int_0^q T_{y10}(q)dq dq dq dq = S'''_{10 \times 10} T_{y10}(q) + \hat{T}'''_{y10}(q),$$

where

$$S''' = \begin{bmatrix} 0 & 0 & 0 & 0 & \frac{1}{72} & 0 & 0 & 0 & 0 & 0 \\ 0 & 0 & 0 & 0 & 0 & \frac{23}{5285} & 0 & 0 & 0 & 0 \\ 0 & 0 & 0 & 0 & 0 & 0 & \frac{29}{16834} & 0 & 0 & 0 \\ 0 & 0 & 0 & 0 & 0 & 0 & 0 & \frac{41}{50415} & 0 & 0 \\ 0 & 0 & 0 & 0 & 0 & 0 & 0 & 0 & \frac{16}{36943} & 0 \\ 0 & 0 & 0 & 0 & 0 & 0 & 0 & 0 & 0 & \frac{19}{75512} \\ 0 & 0 & 0 & 0 & 0 & 0 & 0 & 0 & 0 & 0 \\ 0 & 0 & 0 & 0 & 0 & 0 & 0 & 0 & 0 & 0 \\ 0 & 0 & 0 & 0 & 0 & 0 & 0 & 0 & 0 & 0 \\ 0 & 0 & 0 & 0 & 0 & 0 & 0 & 0 & 0 & 0 \end{bmatrix}, \text{ and } \hat{T}'''_{y10}(q) = \begin{bmatrix} 0 \\ 0 \\ 0 \\ 0 \\ 0 \\ \frac{11}{70463}\xi_{1,11}(q) \\ \frac{6}{58843}\xi_{1,12}(q) \\ \frac{8}{115253}\xi_{1,13}(q) \\ \frac{13}{265929}\xi_{1,14}(q) \end{bmatrix}.$$

Similarly, for repeated integration, we get a higher-order operational integration matrix.

#### 4. METHOD OF SOLUTION

In order to convert the semi-infinte interval  $[0, \infty)$  to the finite interval  $[0,1]$ , we make use of the transformation  $\delta = \frac{\eta}{\eta_\infty}$  and  $F(\delta) = \frac{f(\eta)}{\eta_\infty}$ , and we obtain

$$\eta_\infty^2 \left( F'^2 - FF'' - 2\gamma F''^2 + \left( M \sin^2(\tau) + Da^{-1} \right) F' \right) - F''' - \beta \left( 2F'F''' - FF'''' + 3F''^2 \right) = 0, \tag{4.1}$$

where corresponding boundary constraints are

$$F(0) = 0, \ F'(0) = 1, \ F'(1) = 0, \ \text{and} \ F''(1) = 0. \tag{4.2}$$

Let us assume that

$$F''''(\delta) = G^T T_{y10}(\delta), \tag{4.3}$$

where  $G^T = [g_1, g_2, g_3, g_4, g_5, g_6, g_7, g_8, g_9, g_{10}]$ .

Integrating Eq. (4.3) with respect to  $\delta$

$$F'''(\delta) = F'''(0) + G^T [\hat{T}_{y10}(\delta) + ST_{y10}(\delta)]. \tag{4.4}$$



Integrating Eq. (4.4) with respect to  $\delta$

$$F''(\delta) = F''(0) + \delta F'''(0) + G^T [\hat{T}_{y10}(\delta) + S'T_{y10}(\delta)]. \tag{4.5}$$

Integrating Eq. (4.5) with respect to  $\delta$  and substituting  $F'(0) = 1$ , we get

$$F'(\delta) = 1 + \delta F''(0) + \frac{\delta^2}{2} F'''(0) + G^T [\hat{T}'_{y10}(\delta) + S''T_{y10}(\delta)]. \tag{4.6}$$

Integrating Eq. (4.6) with respect to  $\delta$  and substituting  $F(0) = 0$ , we have

$$F(\delta) = \delta + \frac{\delta^2}{2} F''(0) + \frac{\delta^3}{6} F'''(0) + G^T [\hat{T}''_{y10}(\delta) + S'''T_{y10}(\delta)]. \tag{4.7}$$

Substituting  $\delta = 1$  in Eqs. (4.5) and (4.6), we get

$$F''(1) = F''(0) + F'''(0) + G^T [\hat{T}'_{y10}(\delta) + S'T_{y10}(\delta)]|_{\delta=1}, \tag{4.8}$$

$$0 = F''(0) + F'''(0) + G^T [\hat{T}'_{y10}(\delta) + S'T_{y10}(\delta)]|_{\delta=1}, \tag{4.9}$$

$$F'(1) = 1 + F''(0) + \frac{1}{2} F'''(0) + G^T [\hat{T}''_{y10}(\delta) + S''T_{y10}(\delta)]|_{\delta=1},$$

$$0 = 1 + F''(0) + \frac{1}{2} F'''(0) + G^T [\hat{T}''_{y10}(\delta) + S''T_{y10}(\delta)]|_{\delta=1}. \tag{4.10}$$

Solving Eqs. (4.9) and (4.10), we get

$$F'''(0) = 2 \left[ 1 + G^T [\hat{T}_{y10}(\delta) + S''T_{y10}(\delta)]|_{\delta=1} - G^T [\hat{T}'_{y10}(\delta) + S'T_{y10}(\delta)]|_{\delta=1} \right], \tag{4.11}$$

$$F''(0) = - \left[ 2 \left[ 1 + G^T [\hat{T}''_{y10}(\delta) + S''T_{y10}(\delta)]|_{\delta=1} - G^T [\hat{T}'_{y10}(\delta) + S'T_{y10}(\delta)]|_{\delta=1} \right] + G^T [\hat{T}'_{y10}(\delta) + S'V(\delta)]|_{\delta=1} \right], \tag{4.12}$$

Now, substituting  $F(\delta)$ ,  $F'(\delta)$ ,  $F''(\delta)$ ,  $F'''(\delta)$ , and  $F''''(\delta)$  into the momentum equation, we get a system of nonlinear equations. The unknown coefficients are found by using the collocating points  $\delta_i = \frac{2i-1}{2N}$ , where  $i = 1, 2, 3, \dots$ .

Substitute the obtained coefficient values in Eq. (4.3) to Eq. (4.8) to get numerical solutions to Eqs. (4.1) and (4.2). By substituting the transformation, we get a numerical solution to Eqs. (2.11) and (2.12).

The local skin friction is given by

$$F''(0) = -(1 - 3\beta) \left[ 2 \left[ 1 + G^T [\hat{T}''_{y10}(\delta) + S''T_{y10}(\delta)]|_{\delta=1} - G^T [\hat{T}'_{y10}(\delta) + S'T_{y10}(\delta)]|_{\delta=1} \right] + G^T [\hat{T}'_{y10}(\delta) + S'T_{y10}(\delta)]|_{\delta=1} \right], \tag{4.13}$$

substituting  $F''(0) = \delta_\infty f''(0)$ ,

$$f''(0) = - \frac{1 - 3\beta}{\delta_\infty} \left[ 2 \left[ 1 + G^T [\hat{T}''_{y10}(\delta) + S''T_{y10}(\delta)]|_{\delta=1} - G^T [\hat{T}'_{y10}(\delta) + S'T_{y10}(\delta)]|_{\delta=1} \right] + G^T [\hat{T}'_{y10}(\delta) + S'T_{y10}(\delta)]|_{\delta=1} \right]. \tag{4.14}$$

### 5. NUMERICAL IMPLEMENTATION

$F''''(\delta)$ ,  $F'''(\delta)$ ,  $F''(\delta)$ , and  $F(\delta)$  using the Taylor wavelet method at  $V = 10$  are investigated numerically for MHD Rivlin-Ericksen fluid flow. The parameters that fixed are  $\beta = 0.4$ ,  $\gamma = 0.2$ ,  $M = 5$ ,  $\tau = \pi/4$ , and  $Da^{-1} = 5$ . We get the unknown coefficients as follows:

$$g_1 = \frac{36737}{94}, \quad g_2 = \frac{-66876}{5}, \quad g_3 = \frac{320063}{3}, \quad g_4 = -423616, \quad g_5 = 960579,$$

$$g_6 = -1246922, \quad g_7 = 787999, \quad g_8 = \frac{-4639}{130}, \quad g_9 = -284194, \quad g_{10} = 112613.$$



TABLE 1. Comparison of skin friction coefficient by the Taylor wavelet method with bvp4c for  $\tau = \pi/4$  and  $Da^{-1} = 5$ .

$M$	$\beta$	$\gamma$	$-(1-3\beta)f''(0)$ by the Taylor wavelet method	$-(1-3\beta)f''(0)$ by bvp4c
1	1	1	-1.97892200	-1.97838391
2	1	1	-2.05319515	-2.05278039
2	2	1	-4.06853807	-4.06433668
2	2	2	-3.73329571	-3.73633766

TABLE 2. Comparison of  $f''(0)$  by the Taylor wavelet method with the exact solution for  $\beta = \gamma = 0$ .

$M$	$\tau$	$Da^{-1}$	$f''(0)$ by the Taylor wavelet method	$f''(0)$ by the exact solution
0	0	0	-0.9999353093	-1
1	$\pi/2$	1	-1.73206586515	-1.7320508075
2	$\pi/3$	2	-2.12154605898	-2.1213203435
3	$\pi/4$	3	-2.34506229156	-2.3452078799

On substituting these unknown values in Eq. (4.3) to Eq. (4.8), we get  $F''''(\delta)$ ,  $F'''(\delta)$ ,  $F''(\delta)$ ,  $F'(\delta)$ , and  $F(\delta)$ . From the obtained  $F''''(\delta)$ ,  $F'''(\delta)$ ,  $F''(\delta)$ ,  $F'(\delta)$ , and  $F$  and the coordinate transformations, we obtain  $f''''(\eta)$ ,  $f'''(\eta)'$ ,  $f''(\eta)$ ,  $f'(\eta)$ , and  $f(\eta)$ .

$$\begin{aligned}
F'(\delta) = & \frac{3941455\delta^{12}}{10599} - \frac{2415649\sqrt{23}\delta^{11}}{9788} - \frac{4639\sqrt{21}\delta^{10}}{462540} + \frac{38611951\sqrt{19}\delta^9}{29856} \\
& - \frac{46136114\sqrt{17}\delta^8}{15455} + \frac{14728878\sqrt{15}\delta^7}{4157} - \frac{2038652\sqrt{13}\delta^6}{787} \\
& + \frac{652505335849112947\sqrt{11}\delta^5}{544292615487488} - \frac{1304082\delta^4}{1351} + \frac{9367935\sqrt{7}\delta^3}{380512} \\
& + \frac{4188283895830649\delta^2}{450359962737049} - \frac{7722616686622037\delta}{4503599627370496} + 1, \tag{5.1}
\end{aligned}$$

$$\begin{aligned}
F(\delta) = & \frac{1218616764994167560247\sqrt{3}\delta^{13}}{73786976294838206464} - \frac{227432430621494100295\delta^{12}}{2305843009213693952} \\
& - \frac{13917\sqrt{23}\delta^{11}}{3824795} + \frac{8667989\sqrt{21}\delta^{10}}{70463} - \frac{11845759\sqrt{19}\delta^9}{37756} + \frac{15369264\sqrt{17}\delta^8}{36943} \\
& - \frac{17368256\sqrt{15}\delta^7}{50415} + \frac{212614098198025567\sqrt{13}\delta^6}{1156823671373824} - \frac{1538148\sqrt{11}\delta^5}{26425} + \frac{36737\delta^4}{2256} \\
& + \frac{4188283895830649\delta^3}{13510798882111488} - \frac{7722616686622037\delta^2}{9007199254740992} + \delta. \tag{5.2}
\end{aligned}$$

**Result validation.** In the present study, we apply the Taylor wavelet collocation method to obtain a solution for differential equation (2.7) and compare the solution obtained with the bvp4c in Table 1, thus validating the results so obtained. Results are expressed in the form of graphs for various parameters at  $\beta = 0.4$ ,  $\gamma = 0.2$ ,  $M = 5$ ,  $Da^{-1} = 5$ , and  $\tau = \pi/4$ . Axial velocity and transverse  $f_\eta(\eta)$  and  $f(\eta)$  are achieved by substituting the coordinate transformation  $\delta = \frac{\eta}{\eta_\infty}$  in Eqs. (5.1) and (5.2). With the help of the Taylor wavelet operational matrix, we obtain the local skin friction and is compare it with bvp4c that can be visualized through Table 1.



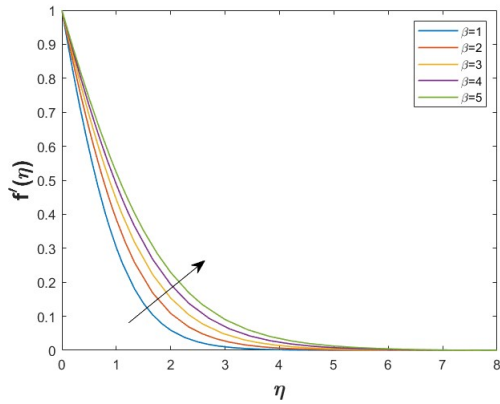


FIGURE 2. Variation of axial velocity for different values of  $\beta$ .

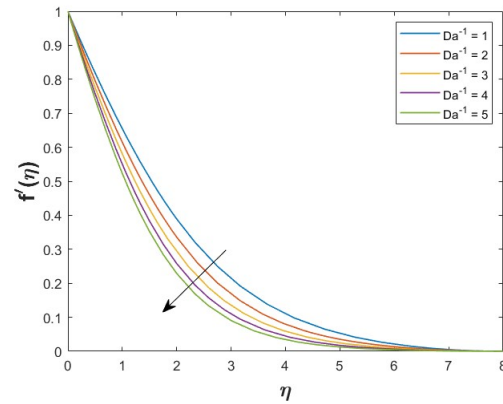


FIGURE 3. Variation of axial velocity for different values of inverse Darcy number.

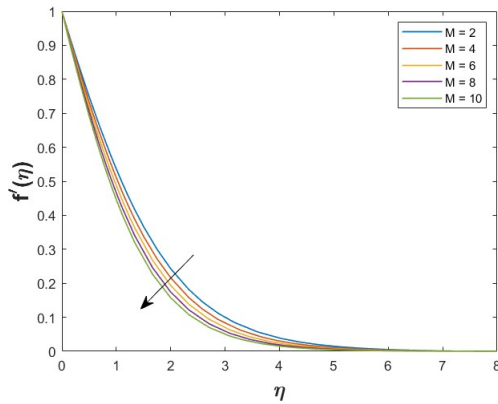


FIGURE 4. Variation of axial velocity for different values of magnetic parameter.

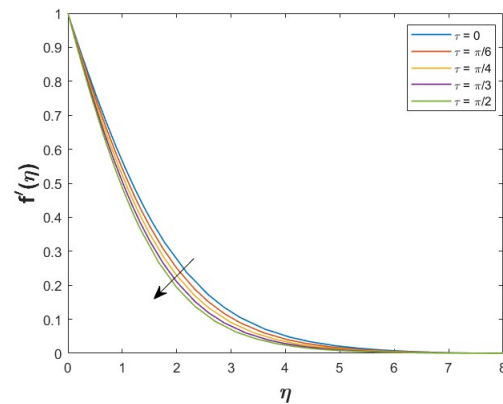


FIGURE 5. Variation of axial velocity for different values of angle of inclination.

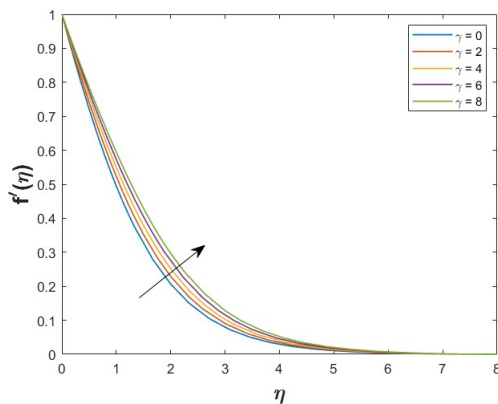


FIGURE 6. Variation of axial velocity for different values of  $\gamma$ .

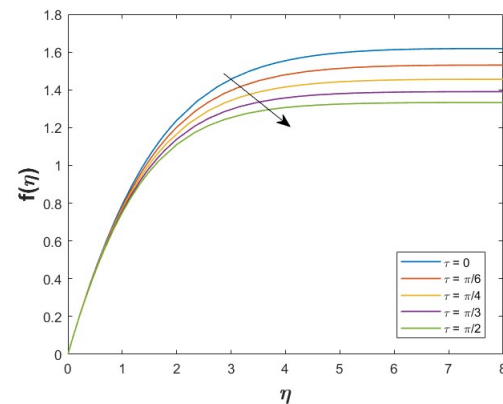


FIGURE 7. Variation of transverse velocity for different values of angle of inclination.



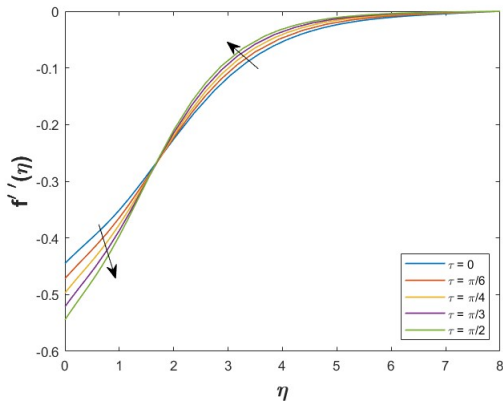


FIGURE 8. Variation of velocity gradient for different values of angle of inclination.

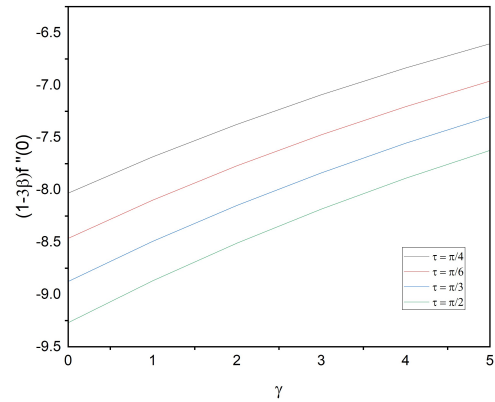


FIGURE 9. Variation of skin friction with respect to  $\gamma$  for different values of  $\tau$ .

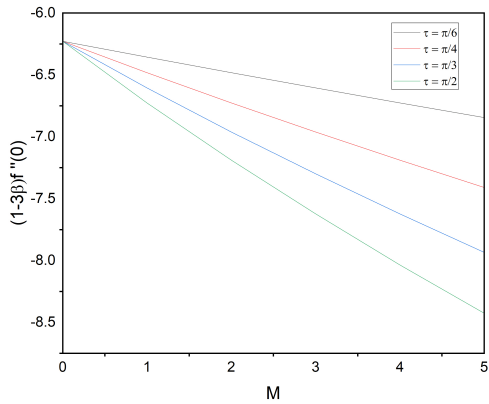


FIGURE 10. Variation of skin friction with respect to  $M$  for different values of  $\tau$ .

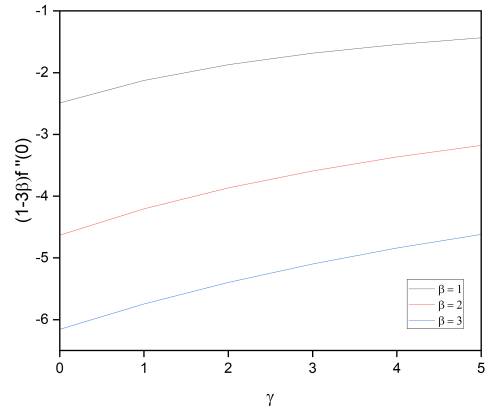


FIGURE 11. Variation of skin friction with respect to  $\gamma$  for different values of  $\beta$ .

TABLE 3. Comparison of  $f''(0)$  by the Taylor wavelet method with Akbar *et al.* [1] for  $\beta=\gamma=Da^{-1}=0$  and  $\tau = \pi/2$ .

$M$	$f''(0)$ by the Taylor wavelet method	$f''(0)$ by Akbar <i>et al.</i> [1]
0	-0.9999353093	-1
1	-1.4148832238	-1.41421
5	-2.44918240569	-2.44949
10	-3.31697827	-3.31663



### 6. EXACT SOLUTION

We obtain the exact solution for  $\beta = \gamma = 0$ ; the equation reduces to

$$f''' + ff'' - f'^2 - (M\sin^2(\tau) + Da^{-1})f' = 0, \tag{6.1}$$

subject to boundary conditions

$$f(0) = 0, \quad f'(0) = 1, \quad \text{and} \quad f'(\infty) \rightarrow 0, \tag{6.2}$$

we obtain solution as

$$f(\eta) = \frac{1 - \exp^{-\eta\sqrt{M\sin^2\tau + Da^{-1} + 1}}}{\sqrt{M\sin^2\tau + Da^{-1} + 1}}. \tag{6.3}$$

Thus,

$$f''(0) = -\sqrt{M\sin^2\tau + Da^{-1} + 1}. \tag{6.4}$$

### 7. RESULTS AND DISCUSSIONS

It can be observed that the axial velocity decreases along  $\eta$  due to the decline of friction from the stretching surface. From Figure 2 it is clear that an increased viscoelastic parameter increases the axial velocity due to the elastic property of the fluid. An increase in the inverse Darcy number decreases the axial velocity due to the porosity of the stretching sheet, as seen in Figure 3.

From Figure 4, it can be observed that an increase in the magnetic field leads to a decrease in the axial velocity because the magnetic field retards the fluid flow making the fluid to flow slowly. Orientation of the magnetic field also plays a vital role in controlling the fluid flow; from Figure 5, it could be observed that as the inclination of the magnetic field is increased from 0 to  $\pi/2$ , the axial velocity decreases. An increase in the cross viscous parameter increases the axial velocity, as seen in Figure 6.

The effect of the angle of inclination on transverse velocity is depicted in Figure 7; it could be concluded that an increase in  $\tau$  decreases the transverse velocity.

From Figure 8, it is clear that the distribution of velocity gradient decreases for an increase in the angle of inclination within the boundary layer, and further, that an increase in the angle of inclination increases the distribution of velocity gradient.

The influence of various parameters on the local skin friction coefficient is depicted in Figures 9-11. In Figure 9, the variation of the local skin friction coefficient with respect to  $\gamma$  for various values of  $\tau$  is studied; it is clear that an increase in  $\tau$  numerically increases the local skin friction. In Figure 10, the variation of the local skin friction coefficient with respect to  $M$  for various values of  $\tau$  is depicted. It could be noted that an increase in  $\tau$  numerically increases the local skin friction coefficient. Further, in Figure 11, the variation of local skin friction coefficient with respect to  $\gamma$  is studied for various values of  $\beta$ , and it could be inferred that an increase in  $\beta$  numerically increases the local skin friction coefficient.

In Table 1, a comparison of the local skin friction coefficient for various values of  $M$ ,  $\beta$ , and  $\gamma$  with `bvp4c` is done. It could be inferred that local skin friction coefficient values by the Taylor wavelet method have a clear agreement with `bvp4c` with very little error.

### 8. CONCLUSION

The Taylor wavelet operational matrix approach has been developed to investigate Revlin-Ericksen fluid moving across a stretching sheet in the vicinity of a magnetic field. The mentioned computational method is utilized to handle boundary-valued nonlinear ordinary differential equations, and the solution obtained via this method has a clear agreement with the values obtained via `bvp4c` with very little error in the solution. The results of the present investigation are presented in an assortment of graphs and tables.

- Axial velocity propels with a rise in the cross viscous parameter and viscoelastic parameter.
- The axial velocity drops as the inverse Darcy number, magnetic field, and inclination angle grow.
- Table 1 and the figures show the way local skin friction alters with different parameters.



## REFERENCES

- [1] N. S. Akbar, A. Ebaid, and Z. H. Khan, *Numerical analysis of magnetic field effects on Eyring-Powell fluid flow towards a stretching sheet*, Journal of magnetism and Magnetic Materials, 382 (2015), 355-358.
- [2] R. Chand and G. C. Rana, *Thermal Instability of Rivlin-Ericksen elastico-viscous nanofluid saturated by a porous medium*, Journal of fluids engineering, 134(12) (2012), 121203.
- [3] L. J. Crane, *Flow past a stretching plate*, Z. Angew Math. Phys., 21 (1970), 645.
- [4] N. Dalir, *Numerical study of entropy generation for forced convection flow and heat transfer of a Jeffrey fluid over a stretching sheet*, Alexandria Engineering Journal, 53(4) (2014), 769-778.
- [5] D. Dharamendra, M. K. Awasthi, V. Kumar, A. Chauhan, and N. Dhiman, *Study of instability of Rivlin-Ericksen viscoelastic fluid film*, AIP Conference Proceedings, AIP Publishing., 2481(1) (2022).
- [6] S. Gümgüm, *Taylor wavelet solution of linear and nonlinear Lane-Emden equations*, Applied Numerical Mathematics, 158 (2020), 44-53.
- [7] U. Gupta, P. Aggarwal, and K. R. Wanchoo, *Thermal convection of dusty compressible Rivlin-Ericksen viscoelastic fluid with Hall currents*, Thermal Science, 16(1) (2012), 177-192.
- [8] P. M. Jordan and P. Puri, *Stokes' first problem for a Rivlin-Ericksen fluid of second grade in a porous half-space*, International Journal of Non-Linear Mechanics, 38(7) (2003), 1019-1025.
- [9] R. A. Kareem, S. O. Salawu, and Y. Yan, *Analysis of transient Rivlin-Ericksen fluid and irreversibility of exothermic reactive hydromagnetic variable viscosity*, J. Appl. Comput. Mech., 6(1) (2020), 26-36.
- [10] E. Keshavarz, Y. Ordokhani, and M. Razzaghi, *The Taylor wavelets method for solving the initial and boundary value problems of Bratu-type equations*, Applied Numerical Mathematics, 128 (2018), 205-216.
- [11] P. Kumar, H. Mohan, and R. Lal, *Effect of magnetic field on thermal instability of a rotating Rivlin-Ericksen viscoelastic fluid*, Int. J. Math. Math. Sci., 2006(3) (2006), 1-10.
- [12] P. A. Kumar and G. J. Singh, *Stability of two superposed Rivlin-Ericksen viscoelastic fluids in the presence of suspended particles*, Romanian Journal of Physics, 51(9) (2006), 927-935.
- [13] S. Kumbinarasaiah and K. R. Raghunatha, *The applications of Hermite wavelet method to nonlinear differential equations arising in heat transfer*, International Journal of Thermofluids, 9 (2021), 100066.
- [14] G. Manohara and S. Kumbinarasaiah, *An innovative Fibonacci wavelet collocation method for the numerical approximation of Emden-Fowler equations*, Applied Numerical Mathematics, 201 (2024), 347-369.
- [15] G. M. Moatimid and A. Sayed, *Nonlinear EHD stability of a cylindrical interface separating two Rivlin-Ericksen fluids: A novel analysis*, Chinese Journal of Physics, 87 (2024), 379-397.
- [16] V. Ramareddy, P. M. Basawaraj, U. S. Mahabaleshwar, and B. Souayeh, *An MHD boundary layer flow of Casson fluid due to a moving wedge analyzed by the Bernoulli wavelet method*, ZAMM-Journal of Applied Mathematics and Mechanics/Zeitschrift für Angewandte Mathematik und Mechanik, (2024), e202300648.
- [17] B. V. Rathish Kumar and M. Mehra, *Wavelet-Taylor Galerkin method for the Burgers equation*, BIT Numerical Mathematics, 45 (2005), 543-560.
- [18] P. C. Reddy, M. C. Raju, G. S. S. Raju, and C. M. Reddy, *Diffusion thermo and thermal diffusion effects on MHD free convection flow of Rivlin-Ericksen fluid past a semi infinite vertical plate*, Bulletin of Pure and Applied Sciences-Mathematics and Statistics, 36(2) (2017), 266-284.
- [19] R. S. Rivlin and J. L. Ericksen, *Stress-deformation relations for isotropic materials*, Collected Papers of RS Rivlin, I-II (1997), 911-1013.
- [20] M. N. Sadiq, M. Sajid, T. Javed, and N. Ali, *A numerical study for heat and fluid flow of couple stress fluid over a spiraling disk by Legendre wavelet spectral collocation method*, ZAMM-Journal of Applied Mathematics and Mechanics/Zeitschrift für Angewandte Mathematik und Mechanik, 100(8) (2020), e201900220.
- [21] R. C. Sharma and P. Kumar, *Effect of rotation on thermal instability in Rivlin-Ericksen elastico-viscous fluid*, Zeitschrift für Naturforschung, 51(7) (1996), 821-824.
- [22] V. Sharma, K. Kishor, and G. Rana, *The instability of streaming Rivlin-Ericksen fluids in porous medium*, Studia Geotechnica et Mechanica, 23(3-4) (2001), 83-93.
- [23] S. C. Shiralashetti and S. I. Hanaji, *Taylor wavelet collocation method for Benjamin-Bona-Mahony partial differential equations*, Results in Applied Mathematics, 9 (2021), 100139.



- [24] A. K. Shukla and M. K. Awasthi, *Stability characteristics of planar Rivlin–Ericksen fluid interface with mass and heat transfer*, Journal of Fluids Engineering, *145*(3) (2023), 031302.
- [25] B. Siddappa and P. S. Hiremath, *Rivlin–Ericksen fluid flow past a stretching plate with suction*, Kyungpook Mathematical Journal, *20*(2) (1980), 267–272.
- [26] B. Siddappa and B. S. Khapate, *Rivlin–Ericksen fluid flow past a stretching plate*, Rev. Roum. Sci. Techn. -Mec. Appl., *21* (1976), 497–505.
- [27] M. Slemrod, *Constitutive Relations for Rivlin–Ericksen Fluids Based on Generalized Rational Approximation*, Archive for rational mechanics and analysis, *146*(1) (1999), 73–93.
- [28] P. T. Toan, T. N. Vo, and M. Razzaghi, *Taylor wavelet method for fractional delay differential equations*, Engineering with Computers, *37*(1) (2021), 231–240.
- [29] R. Vidya Shree, B. Patil Mallikarjun, and A. J. Chamkha, *Analysis of MHD boundary layer flow of a viscous fluid past a stretching sheet employing the Legendre wavelet method*, International Journal of Ambient Energy, *45*(1) (2024), 2310629.
- [30] R. Vidya shree, B. Patil Mallikarjun, and S. Kumbinarasaiah, *Entropy generation on an MHD Casson fluid flow in an inclined channel with a permeable walls through Hermite wavelet method*, Results in Control and Optimization, *12* (2023), 100261.
- [31] R. Vidya Shree, B. Patil Mallikarjun, and S. Kumbinarasaiah, *Time-varying stretching velocity analysis for an unsteady flow of Williamson fluid by Hermite wavelet*, Journal of Umm Al-Qura University for Applied Sciences, *10*(3) (2024), 541–554.
- [32] A. B. Vishalakshi, U. S. Mahabaleshwar, and Y. Sheikhnejad, *Impact of MHD and mass transpiration on Rivlin–Ericksen liquid flow over a stretching sheet in a porous media with thermal communication*, Transport in Porous Media, *142*(1) (2022), 353–381.
- [33] Vivek and M. Kumar, *Bernoulli wavelet application to the numerical solution of Jeffery–Hamel flow problem*, Numerical Heat Transfer, Part B: Fundamentals, *86*(6) (2025), 1867–1886.

